Received: 13 July 2022 | Revised: 22 August 2022 | Accepted: 6 September 2022

DOI: 10.1111/cas.15578

Cancer Science WILEY

ORIGINAL ARTICLE

N6-methyladenosine-modified HOTAIRM1 promotes vasculogenic mimicry formation in glioma

Zhangyi Wu[1] | Yihai Lin[1] | Nan Wei[2]

[1]Department of Neurosurgery, Zhejiang Provincial Tongde Hospital, Hangzhou, China

[2]Department of Oncology, Zhejiang Hospital, Hangzhou, China

Correspondence
Nan Wei, Department of Oncology, Zhejiang Hospital, No. 12 Lingyin Road, Hangzhou, Zhejiang 310013, China.
Email: wenan_edu@hotmail.com

Yihai Lin, Department of Neurosurgery, Zhejiang Provincial Tongde Hospital, No. 234 Gucui Road, Hangzhou, Zhejiang 310012, China.
Email: 201823210201028@zcmu.edu.cn

Funding information
Zhejiang Basic Public Welfare Research Program, Grant/Award Number: LGF22H160067

Abstract

Vasculogenic mimicry (VM) has been reported to accelerate angiogenesis in malignant tumors, yet the mechanism underlying VM has not been fully elucidated. N6-methyladenosine (m6A) mainly modulates mRNA fate and affects multiple tumorigenesis. Here, we aimed to investigate m6A-modified HOXA transcript antisense RNA myeloid-specific 1 (HOTAIRM1) in the regulation of glioma-associated VM formation. Gene expression was analyzed by quantitative RT-PCR. Cell viability, metastases, and VM formation capacity were determined by CCK-8, migration and invasion, as well as tube formation assays, respectively. The function and mechanisms of m6A-modified HOTAIRM1 were defined through liquid chromatography–tandem mass spectrometry m6A quantification, methylated RNA immunoprecipitation sequencing, RNA stability assays, and RNA pull-down experiments. A glioma xenograft mouse model was further established for VM evaluation in vivo. The results showed that HOTAIRM1, methyltransferase-like 3 (METTL3), and insulin-like growth factor binding protein 2 (IGFBP2) were upregulated in glioma tissues and cell lines. HOTAIRM1 functions as an oncogene in glioma progression; however, knockdown of HOTAIRM1 significantly reduced cell viability, migration, invasion, and VM formation. Notably, METTL3-dependent m6A modification enhanced HOTAIRM1 mRNA stability, whereas knockdown of METTL3 deficiency significantly suppressed VM in glioma. Moreover, HOTAIRM1 was found to bind IGFBP2, and HOTAIRM1 deficiency blocked glioma progression and VM formation in vivo. Our results indicated that METTL3-dependent m6A-modified HOTAIRM1 promoted VM formation in glioma.

KEYWORDS
Glioma, HOTAIRM1, IGFBP2, METTL3, N6-methyladenosine, vasculogenic mimicry

Abbreviations: ADAM, a disintegrin and metalloproteinase; HOTAIRM1, HOXA transcript antisense RNA myeloid-specific 1; IGFBP2, insulin-like growth factor binding protein 2; LC-MS/MS, liquid chromatography–tandem mass spectrometry; lncRNA, long noncoding RNA; m6A, N6-methyladenosine; MeRIP, methylated RNA immunoprecipitation sequencing; METTL3, methyltransferase-like 3; ncRNA, noncoding RNA; NHA, normal human astrocyte; qRT-PCR, quantitative RT-PCR; RBP, RNA binding protein; ROC, receiver operating characteristic; SRAMP, sequence-based RNA adenosine methylation site predictor; VM, vasculogenic mimicry.

1 | INTRODUCTION

Gliomas are the most frequent type of primary intracranial neoplasm of the central nervous system, leading to significantly high morbidity, relapse rates, and mortality worldwide annually.[1,2] Malignant glioma cases can almost invariably recur, mainly due to their invasiveness and resistance to standard chemo- or radiotherapy.[3,4] Gliomas have been histologically classified according to both major characteristics, cell proliferation and angiogenesis.[5,6] Angiogenesis has been revealed to be especially crucial for the transition of gliomas from low-grade to high-grade, and moreover, it is generally accepted that a significant and direct correlation exists between the extent of vascularization and increased malignancy.[7]

Vasculogenic mimicry was first described in uveal melanomas by Maniotis et al. in 1999 and later defined as the developmental structure of microvascular channels derived from metastatic, aggressive, or genetically dysfunctional tumor cells.[8–10] The distinctive two types of VM (tubular and patterned) have been extensively reported in various tumors, such as colorectal cancer, breast cancer, ovarian cancer, hepatocellular carcinoma, and gliomas.[11–16] Fortunately, research and development of novel drugs based on the VM theory promises potential for cancer treatment. Among them, versatile functions and linkages between N6-methyladenosine (m6A) and multiple tumor types have been reported in cases that include breast cancer, kidney cancer, gastric cancer, leukemia, mesothelioma, pancreatic cancer, sarcoma, and prostate cancer.[17–24] However, to date, only a few studies have discussed m6A-associated VM formation in hepatocellular carcinoma,[25] colorectal cancer,[26] and glioblastoma.[27] Research on the potential relationship between m6A modification and VM formation in various cancer types is still far from sufficient.

The m6A modification is an internal modification of mRNAs and ncRNAs widely conserved among eukaryotes.[28] Methyltransferase-like 3 is an m6A writer that plays a key role in m6A methylation.[29,30] Previous studies have revealed that METTL3 expression is dysregulated in cancer via diverse mechanisms, and METTL3 functions as an m6A methyltransferase in cancer.[31] It promotes the progression of various cancers, including gastric cancer, colorectal carcinoma, and glioma.[32–34] HOXA transcript antisense RNA, myeloid-specific 1 is an lncRNA reported to be an oncogene that facilitates proliferation and invasion in thyroid cancer, ovarian cancer, and glioblastoma.[35–37] Abnormal m6A modifications on ncRNAs affect cancer cell proliferation, invasion, and chemoresistance, which suggests a potential association between m6A ncRNA modification and cancer development, and could shed new light on cancer treatment.[38]

In the present study, we focused on the function and regulatory mechanism of HOTAIRM1 on glioma tumor growth, cell migration, invasion, and VM formation in vitro and in vivo. We assumed that HOTAIRM1 promoted VM formation in glioma through METTL3-dependent m6A modification. The findings of our study might provide novel strategies for VM-based glioma treatment.

2 | MATERIALS AND METHODS

2.1 | Bioinformatics analysis

The m6A modification site of HOTAIRM1 was predicted in the SRAMP database (http://www.cuilab.cn/sramp).[39] The potential RBPs for HOTAIRM1 were predicted with StarBase 2.0 software (https://starbase.sysu.edu.cn/starbase2/).[40]

2.2 | Patient and clinical tissues

Glioma tissues were excised from patients suffering from glioma by pathological diagnosis requiring surgical resection. According to the WHO grades, the tumor tissues were classified as low-grade gliomas (WHO I–II, $n = 12$) and high-grade gliomas (WHO III–IV, $n = 12$). The clinical characteristics of the participants in this study are shown in Table 1. Additionally, normal brain tissues were collected from 15 cases of patients undergoing craniocerebral trauma as control specimens. All clinical samples were immediately cryopreserved in liquid nitrogen before RNA extraction.

TABLE 1 Relationship between HOXA transcript antisense RNA myeloid-specific 1 (HOTAIRM1) expression and clinical characteristics of glioma patients

Variable	*n*	HOTAIRM1 expression		*p* value
		High	Low	
Gender				
Male	11	6	5	0.973
Female	13	7	6	
Age, years				
<50	14	8	6	0.521
≥50	10	7	3	
WHO grade				
I–II	12	5	7	0.035
III–IV	12	10	2	
KPS score				
<80	17	13	4	0.028
≥80	7	2	5	
Extent of resection				
Partial	5	3	2	0.769
Total	19	10	9	
Tumor size				
<5 cm	20	12	8	0.711
≥5 cm	4	2	2	

Abbreviation: KPS, Karnofsky Performance Scale.

2.3 | Cell culture and plasmid transfection

The NHA cell line was provided by ScienCell (cat. no. #1800). The human glioma cell line U87 (cat. no. HTB-14) was purchased from ATCC, and the human glioma cell line U251 was provided by Procell Life Science & Technology Co., Ltd. (cat. no. CL-0237). All cell lines were cultured in DMEM containing 10% FBS at 37°C under 5% CO_2. Plasmids designed for target gene knockdown using shRNAs (sh-HOTAIRM1#1#2, sh-METTL3#1#2), rescue assays (sh-HOTAIRM1 + pcDNA-IGFBP2), and negative controls (sh-NC) were all constructed and generated by Sangon Biotech. Lipofectamine 3000 transfection reagent (Thermo Fisher Scientific) was used, and the cells were harvested 48 h posttransfection.

2.4 | Cell viability assay (CCK-8)

Cell proliferation ability was evaluated using CCK-8. Briefly, glioma cell lines (U87 and U251) and normal controls (NHA) were seeded and cultured in 96-well plates at 37°C, and measurements were sequentially carried out at different time points (24 h, 48 h, 72 h, and 96 h). For the cell viability assay, 10 μl CCK-8 reagent solution was added to each well of the plates, and the cells were incubated for another 2 h protected from light. Absorbance intensity was monitored on a microplate reader (Tecan) at 450 nm.

2.5 | Transwell assays

Transwell assays were carried out to examine the migration and invasion abilities of glioma cells after the indicated transfections. Briefly, glioma cell lines (U87 and U251) were diluted in serum-free medium (approximately 1×10^4 cells/well) and seeded into the upper Transwell chamber (BD Biosciences). Meanwhile, the lower chamber was filled with DMEM containing 10% FBS as a chemoattractant. After 48 h of incubation at 37 °C, the migrated cells were fixed in methanol at room temperature and then subjected to 0.1 crystal violet staining. Finally, a minimum of five randomly selected visual fields were randomly chosen and observed under a light microscope to count the number of migrated cells. For cell invasion measurement, the Transwell inserts were coated with Matrigel (280 mg/ml; BD Biosciences) and incubated for 4 h at 37°C. The other procedures were the same as those used for the migration assay.

2.6 | Tube formation assay

The angiogenesis of U87 and U251 cells was measured using tube formation assays. Briefly, 96-well plates were precoated with Matrigel (100 μl; BD Biosciences) for 30 min at 37°C and then the cells were suspended and grown into the plates at 1×10^5 cells/well for 6 h of incubation. Finally, the images were photographed, tubular structures were observed using an inverted microscope (Olympus), and the total number of loops was manually counted.

2.7 | Quantitative RT–PCR

Gene expression levels were analyzed by qRT-PCR. Briefly, total RNA was extracted from either clinical glioma tissues or cell lines using the RNeasy Plus Kit (Qiagen). The cDNA templates were subsequently prepared by reverse transcription using a Reverse Transcription Kit (TaKaRa). The qRT-PCRs were conducted on an ABI 7500 Real-Time PCR System with SYBR Green PCR Master Mix (Applied Biosystems). The PCR cycling program was set and proceeded as follows: activation at 95°C for 10 min, 95°C for 15 s, 48 cycles of (95°C for 15 s, and 60°C for 1 min). All experiments were repeated three times independently. The *GAPDH* gene was used as an internal control. The relative gene expression levels were calculated and normalized according to the $2^{-\Delta\Delta Ct}$ method. The primers used are listed in Table S1.

2.8 | Fluorescence in situ hybridization (FISH)

RNA FISH was carried out using a FISH detection kit (Roche) for subcellular localization of HOTAIRM1. Briefly, glioma cell lines (U87 and U251) were cultured and fixed with 4% paraformaldehyde at room temperature. After washing, the cells were incubated overnight with hybridization solutions containing digoxin-labeled HOTAIRM1 probe. The cell nuclei were then subjected to DAPI staining for 15 min. Finally, the cells were observed, and images were taken under a fluorescence microscope (Olympus, Japan).

2.9 | N6-methyladenosine quantification by LC-MS/MS

Quantification of m6A levels in glioma cell lines (U87 and U251) or NHA controls was undertaken using LC–MS/MS as previously described.[25]

2.10 | Methylated RNA immunoprecipitation

Total RNA was extracted from glioma cell lines (U87 and U251), and rRNAs were subsequently depleted using a Ribosomal RNA Removal Kit (Illumina). The obtained RNA extractions were then sheared into approximately 100-nt fragments using RNA Fragmentation Reagents (AM8740; Invitrogen). Chemically fragmented RNAs were immunoprecipitated with the anti-IgG (control) or anti-m6A Ab using a Magna MeRIP m6A Kit (Millipore) following the manufacturer's instructions. Finally, m6A-enriched RNAs were identified by qRT-PCR analysis.

2.11 | RNA stability assay

Briefly, glioma cell lines (U87 and U251) transfected with shRNAs (sh-METTL3 or sh-NC) were treated with actinomycin D (approximately 5 μg/ml; Sigma-Aldrich) for transcription blockade. After treatment, RNA was extracted at each time point (0, 1, 2, 3, and 4 h) and subjected to qRT-PCR analysis for HOTAIRM1 RNA stability detection.

2.12 | RNA pull-down assay

The RNA pull-down experiments were carried out using a Magnetic RNA–Protein Pull-Down Kit (Thermo Fisher Scientific). Briefly, biotin-labeled IGFB2 (Bio-IGFBP2) and negative control (Bio-NC) probes were coincubated with glioma cell lines at 37°C for 48 h. Then the cells were collected and lysed with lysis buffer at 4°C for 10 min. Next, cell lysates were cultured with streptavidin magnetic beads at 4°C overnight. After washing the beads three times, the bound RNA was extracted using TRIzol reagent (Invitrogen), and the enrichment of HOTAIRM1 was determined by qRT-PCR analysis.

2.13 | Tumor xenograft mouse model establishment and VM detection

All animal experiments were approved by the Ethics Committee of Zhejiang Provincial Tongde Hospital according to the Guidelines for the Care and Use of Laboratory Animals. BALB/c nude mice (4 weeks old, male) were purchased from Vital River Laboratory Animals and maintained under specific pathogen-free conditions. For in vivo tumor xenograft model establishment, 10 mice were randomly chosen and divided into two groups: the sh-NC and sh-HOTAIRM1 groups. Next, U87 cells (approximately 1×10^6/200 μl PBS) transfected with shRNAs (sh-HOTAIRM1 or sh-NC) were subcutaneously inoculated into the right frontal node of nude mice. Tumor growth was monitored once weekly. Mice were killed by cervical dislocation until the fifth week (35 days), and tumors were resected and measured for weight and volume. The samples were then subjected to H&E staining for histopathological examination. Slides were also subjected to immunohistochemistry by the CD31/PAS double staining method for VM detection and scoring.

2.14 | Statistical analysis

All experiments were carried out with at least three independent biological triplicates. Statistical analysis was performed using SPSS 21.0 (SPSS) or GraphPad Prism software (version 8.0). Significant differences were analyzed using Student's *t*-test (between two groups) or ANOVA (among or more than three groups). Receiver operating characteristic analysis was applied to assess the predictive value. Spearman's correlation analysis was carried out to determine the correlation between IGFBP2 and HOTAIRM1 and the correlation between METTL3 and HOTAIRM1 in glioma patient tissues using GraphPad Prism software (version 8.0). The results are presented as the means ± SD. A p value of less than 0.05 was considered statistically significant.

3 | RESULTS

3.1 | HOTAIRM1 functions as an oncogene and is upregulated in glioma tissues and cell lines

To investigate whether HOTAIRM1 functions in glioma progression, we first examined gene expression levels in glioma clinical specimens and different cell lines. The qRT-PCR results shown in Figure 1A,B indicated that HOTAIRM1 was upregulated in both glioma tissues (more significantly expressed in high-grade than low-grade) and different cell lines (more significantly expressed in U251 than U87). Additionally, the gene expression levels of *HOTAIRM1* in glioma cell lines (U251 compared with U87) were further examined and validated by FISH assay (Figure 1D). The ROC curve analysis also revealed a potential diagnostic value of HOTAIRM1 in glioma patients (Figure 1C). These results indicated that *HOTAIRM1* might function as an oncogene and be involved in glioma progression.

3.2 | Knockdown of HOTAIRM1 reduces VM in glioma cells

To further explore whether HOTAIRM1 was associated with VM in glioma, a series of loss-of-function experiments were undertaken in vitro. Knockdown of HOTAIRM1 in an in vitro model was successfully established through shRNA (sh-HOTAIRM1#1#2) transfection and verified by qRT-PCR analysis (Figure 2A). The CCK-8 assays showed that HOTAIRM1 silencing could significantly inhibit glioma cell proliferation and viability (Figure 2B). Additionally, Transwell and tube formation assay results indicated that HOTAIRM1 deviancy dramatically suppressed glioma cell motivations (Figure 2C) and VM formation ability (Figure 2D).

3.3 | METTL3-dependent m6A modification enhances HOTAIRM1 stability in glioma cells

The qRT-PCR results shown in Figure 3A,B indicated that the m6A writer (METTL3) was also significantly and highly expressed in both glioma tissues and cell lines, similar to HOTAIRM1 (Figure 1A,B). Therefore, to clarify whether the m6A modification process is associated with HOTAIRM1 behavior, METTL3 was knocked down in glioma cell lines. The knockdown efficiency of METTL3 was verified using qRT-PCR assays, which revealed that the expression of METTL3 was significantly reduced after the transfection of sh-METTL3#1/#2 in glioma cells (Figure 3C). The qRT-PCR

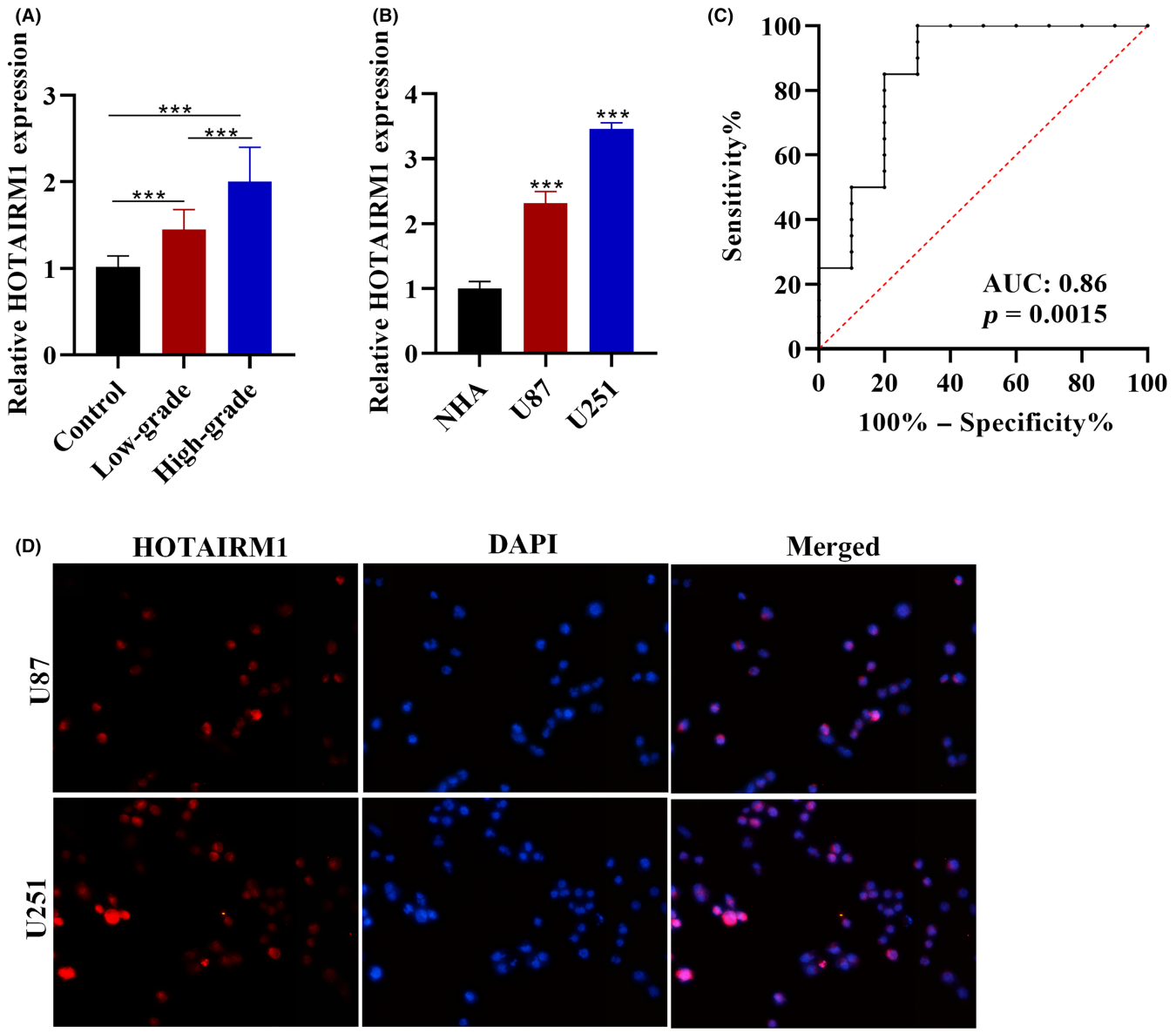

FIGURE 1 HOXA transcript antisense RNA myeloid-specific 1 (HOTAIRM1) functions as an oncogene and is upregulated in glioma tissues and cell lines. Quantitative RT-PCR analysis of HOTAIRM1 expression in (A) glioma tissues and (B) cell lines (U87 and U251). Tumor specimens were classified as low-grade gliomas (WHO I–II, $n = 12$) or high-grade gliomas (WHO III–IV, $n = 12$). Normal brain tissues collected from patients undergoing craniocerebral trauma ($n = 15$) and normal human astrocyte cell lines (NHA) were used as control groups. (C) Diagnostic value of HOTAIRM1 in glioma patients by ROC curve analysis. (D) Gene expression and localization of HOTAIRM1 by FISH detection. Magnification, 200×. ***$p < 0.001$. AUC, area under the receiver operating characteristic curve

results showed that METTL3 silencing led to direct suppression of HOTAIRM1 expression (Figure 3D), indicating that METTL3 is essential for HOTAIRM1 regulation. In addition, LC-MS/MS and qRT-PCR analysis results showed much higher m6A modification mRNA levels in glioma cells (Figure 3E). Moreover, METTL3-dependent m6A modification of HOTAIRM1 was further confirmed by MeRIP analysis (Figure 3F); that is, HOTAIRM1 expression and regulation were modulated by m6A modification in glioma cells. To investigate whether m6A modification might affect HOTAIRM1 stability, an RNA stability assay was undertaken in METTL3-depleted glioma cells versus sh-NC controls using actinomycin D treatment and detection. The results showed that METTL3 deficiency significantly imparted HOTAIRM1 stability in glioma cells (Figure 3G). Consistent results were further revealed based on Spearman's correlation analysis of HOTAIRM1 and METTL3, which revealed that the expression of METTL3 was positively correlated with that of HOTAIRM1 in glioma patient tissues ($r = 0.5574$, $p = 0.0047$) (Figure 3H).

3.4 | METTL3 deficiency suppresses VM in glioma cells

We further investigated whether the m6A writer METTL3 was involved in VM in glioma cells. The CCK-8 assay results showed that METTL3 deficiency significantly suppressed glioma cell viability

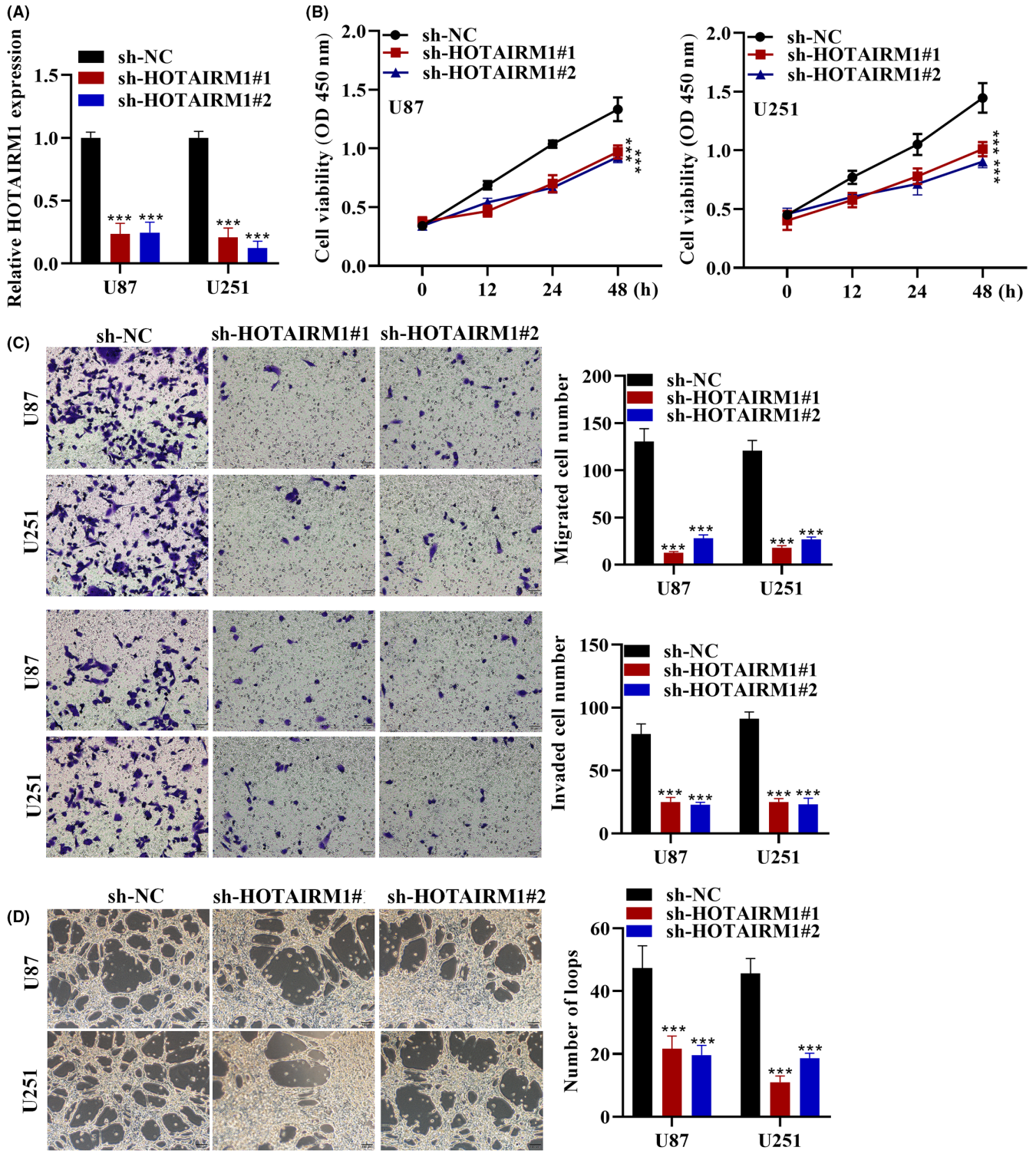

FIGURE 2 Knockdown of HOXA transcript antisense RNA myeloid-specific 1 (HOTAIRM1) reduces vasculogenic mimicry (VM) in glioma cells. (A) Knockdown of HOTAIRM1 in an in vitro model established through cell transfection with shRNAs (sh-HOTAIRM1#1#2) and verified by quantitative RT-PCR. (B) Assessment of HOTAIRM1 deviancy on glioma cell viability and proliferation by CCK-8 assay. (C) Transwell and tube formation assays after HOTAIRM1 silencing. Scale bar, 50 μm. (D) Assessment of the effect of HOTAIRM1 deficiency on VM formation in glioma cells. Scale bar, 100 μm. ***$p < 0.001$. NC, negative control; OD, optical density

and proliferation (Figure 4A). Additionally, Transwell and tube formation assays indicated that METTL3 deviancy significantly inhibited glioma cell motivation (Figure 4B) and VM formation ability (Figure 4C).

3.5 | HOTAIRM1 binds to IGFBP2 mRNA

Based on bioinformatics prediction using StarBase 2.0 software, the sequence of HOTAIRM1 harbored potential binding domains with

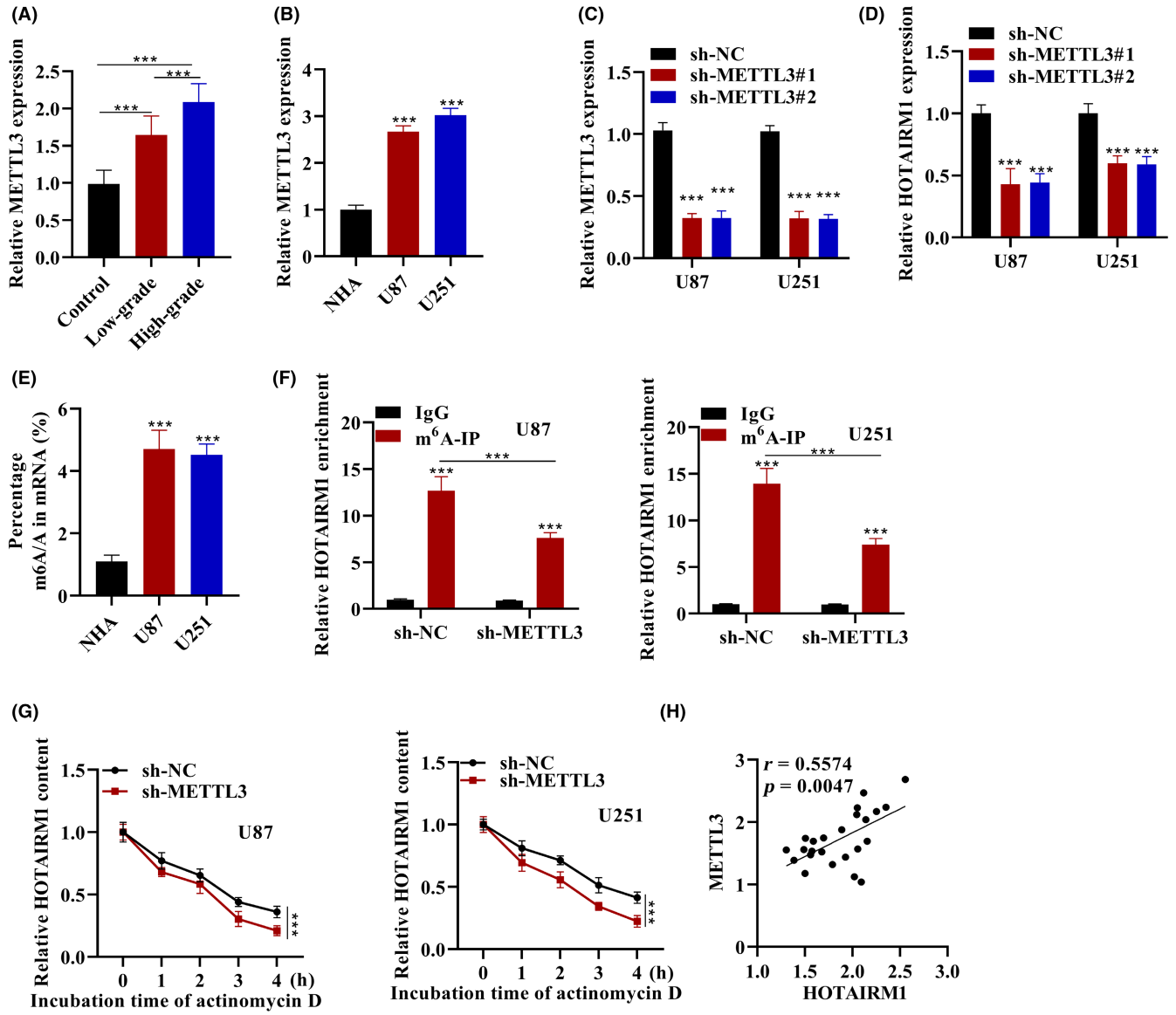

FIGURE 3 Methyltransferase-like 3 (METTL3)-dependent N6-methyladenosine (m6A) modification enhances HOXA transcript antisense RNA myeloid-specific 1 (HOTAIRM1) stability in glioma cells. (A) Quantitative RT-PCR (qRT-PCR) analysis of METTL3 expression in (A) glioma tissues and (B) cell lines (U87 and U251). (C) qRT-PCR analysis of METTL3 and (D) HOTAIRM1 expression in glioma cells after METTL3 knockdown. (E) Quantification of m6A mRNA levels in glioma cell lines (U87 and U251) by liquid chromatography–tandem mass spectrometry and qRT-PCR analysis. (F) m6A-enriched HOTAIRM1 abundance was determined by methylated RNA immunoprecipitation (IP) and qRT-PCR analysis. (G) HOTAIRM1 stability detection by qRT-PCR analysis. (H) Correlation between HOTAIRM1 and METTL3 assessed by Spearman's correlation analysis. ***$p < 0.001$. NC, negative control; NHA, normal human astrocyte

IGFBP2 mRNA (Figure 5A). In addition, IGFBP2 was detected to be highly expressed in glioma tissues and cell lines (Figure 5B,C). We also examined the gene expression change tendency of IGFBP2 after knockdown of HOTAIRM1. The results showed that HOTAIRM1 deficiency led to the direct downregulation of IGFBP2 expression in glioma cells (Figure 5D). To confirm whether HOTAIRM1 binds to IGFBP2 mRNA, we undertook RNA pull-down assays. HOTAIRM1 was abundantly enriched in the IGFBP2 mRNA complex according to the results of RNA pull-down assays (Figure 5E). Moreover, a positive correlation between HOTAIRM1 and IGFBP2 was revealed by Spearman's correlation analysis ($r = 0.4322$, $p = 0.0349$) (Figure 5F).

3.6 | IGFBP2 reversed the effects of HOTAIRM1 deficiency on VM in glioma cells

To further explore the role of IGFBP2 in glioma cells, we undertook gain- and loss-of-function experiments. A rescue assay model was successfully established through glioma cell transfection with shRNAs (sh-HOTAIRM1 + pcDNA-IGFBP2) and verified by qRT-PCR (Figure 6A). Consistent with Figure 2B, HOTAIRM1 deficiency significantly suppressed glioma cell proliferation and viability. However, the inhibition could be reversed by IGFBP2 complementary overexpression in glioma cells (Figure 6B). Likewise, Transwell and tube

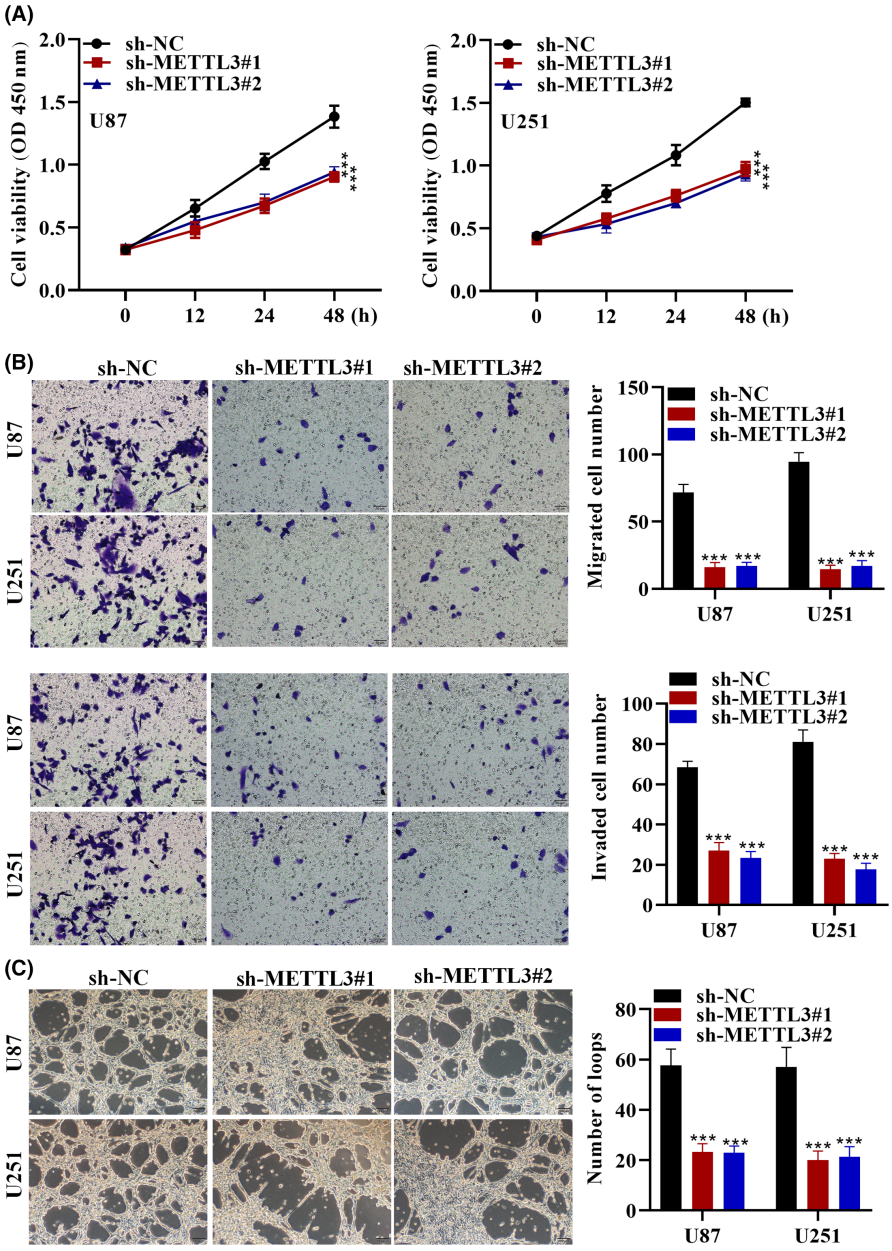

FIGURE 4 Methyltransferase-like 3 (METTL3) deficiency suppresses vasculogenic mimicry (VM) in glioma cells. (A) Assessment of METTL3 deviancy on glioma cell viability and proliferation by CCK-8 assay. (B) Transwell and tube formation assays after METTL3 silencing. Scale bar, 50 μm. (C) Assessment of METTL3 deficiency on VM formation in glioma cells. Scale bar, 100 μm. ***$p < 0.001$. NC, negative control; OD, optical density

formation assay results showed that the effects of HOTAIRM1 deficiency on glioma cell motivation (Figures 2C and 6C) and VM formation ability (Figures 2D and 6D) could be reversed by IGFBP2 rescue.

3.7 | HOTAIRM1 deficiency inhibits glioma progression and VM formation in vivo

Finally, the effects of HOTAIRM1 deficiency on VM in glioma progression were verified in vivo. A glioma xenograft mouse model was successfully established by subcutaneous injection with U87 cells transfected with shRNAs (sh-HOTAIRM1 or sh-NC). As indicated in Figure 7A, glioma xenograft tumors in sh-HOTAIRM1-treated nude mice were markedly restrained. Moreover, tumor growth/volume and weight were significantly lower in sh-HOTAIRM1 mice (Figure 7B,C). In addition, histopathological examination was carried out by H&E staining. Immunohistochemistry assays by the CD31/PAS double staining method were undertaken for VM detection and scoring. The results showed that VM formation and structures were significantly reduced in sh-HOTAIRM1 mice compared to sh-NC mice (Figure 7D,E). These findings suggest that HOTAIRM1 deficiency blocks glioma progression and VM formation in vivo.

4 | DISCUSSION

In the present study, we found that HOTAIRM1 was significantly upregulated in glioma cells and high-grade glioma patient tissues. HOTAIRM1 is of prognostic value for prognosis in glioma patients. Moreover, METTL3-dependent m6A modification enhanced HOTAIRM1 stability and the viability, migration, invasion, and angiogenesis of glioma cells. In vivo assays further indicated that

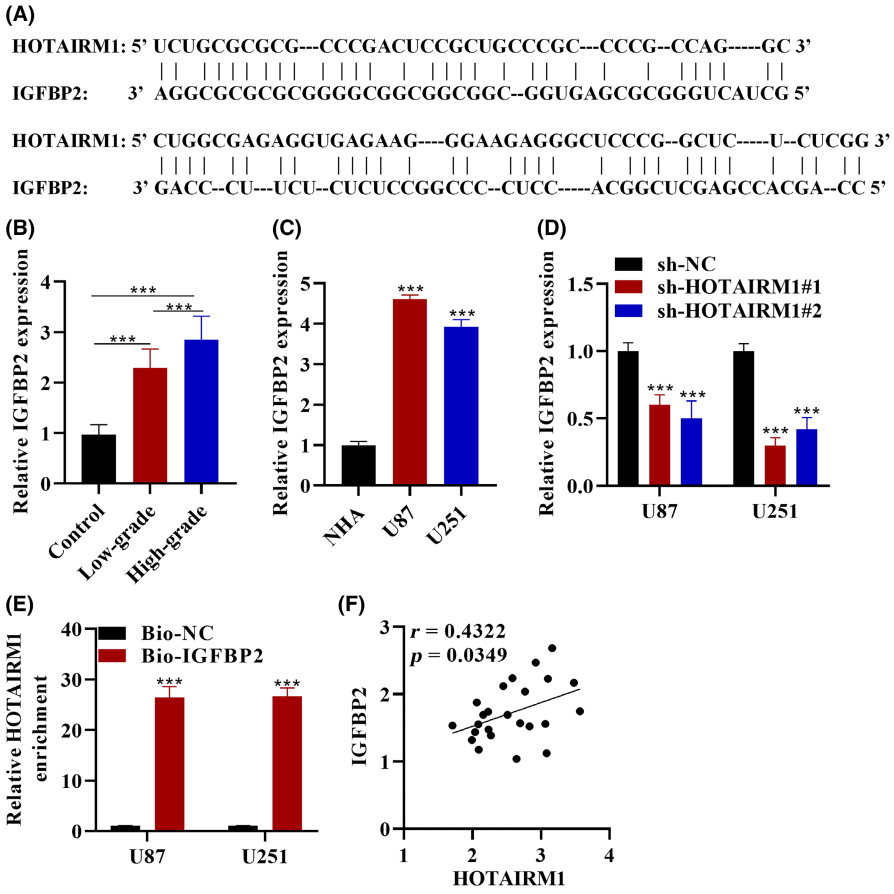

FIGURE 5 HOXA transcript antisense RNA myeloid-specific 1 (HOTAIRM1) binds to insulin-like growth factor binding protein 2 (IGFBP2) mRNA. (A) Sequence of HOTAIRM1 harbored potential binding domains with IGFBP2 mRNA based on StarBase 2.0 bioinformatics prediction. (B, C) Quantitative RT-PCR (qRT-PCR) analysis of IGFBP2 expression in (B) glioma tissues and (C) cell lines (U87 and U251). (D) qRT-PCR analysis of IGFBP2 expression in glioma cells after HOTAIRM1 knockdown. (E) HOTAIRM1 binding to IGFBP2 mRNA was verified by RNA pull-down assay. (F) Correlation between HOTAIRM1 and IGFBP2 assessed by Spearman's correlation analysis. ***$p < 0.001$. Bio-NC, biotin-labeled negative control

HOTAIRM1 knockdown inhibited tumor growth and angiogenesis in glioma.

N6-methyladenosine modification plays a vital role in the initiation and development of different types of cancer through diverse mechanisms.[41,42] Normal m6A levels are usually dramatically altered in a large number of cancers.[43] Reduced m6A levels caused by METTL3/METTL14 downregulation lead to aberrant upregulation and activation of oncogenes, such as ADAM metallopeptidase (e.g., ADAM19),[43–45] which indicates that altered m6A levels and m6A marketed "writers" and "erasers" might serve as potential therapeutic targets for cancer treatment. METTL3-mediated m6A modification is critically involved in glioma progression. For example, YTHDF2 facilitates glioma progression by promoting UBXN1 mRNA decay by METTL3-mediated m6A modification in glioma.[46] Methyltransferase-like 3 promotes the development of IDH-WT gliomas by upregulating MALAT1 through m6A modification.[34] Methyltransferase-like 3 is also indicated to be highly expressed in glioblastoma, and promotes glioblastoma proliferation by upregulating ADAR1 in an m6A-dependent manner.[47] In our study, METTL3 (an m6A writer) was detected to be significantly highly expressed in glioma cells and patient tissues (with more significant upregulation in high-grade groups). The m6A mRNA levels were also revealed to be upregulated in glioma cells. Methyltransferase-like 3 knockdown was shown to significantly inhibit the proliferation, migration, invasion, and angiogenesis of glioma cells, which was consistent with previous studies.

Increasing evidence has revealed that *HOTAIRM1* is an oncogene in glioma that facilitates tumor proliferation and reduces apoptosis and radiosensitivity.[48–50] In our study, HOTAIRM1 was predicted to have an m6A site at very high confidence according to the SRAMP database, and the m6A modification levels of HOTAIRM1 were significantly reduced after METTL3 knockdown in glioma cells. Moreover, the stability of HOTAIRM1 was significantly decreased after silencing METTL3 in glioma cells. According to the Pearson correlation analysis, the expression of HOTAIRM1 and METTL3 was positively correlated in glioma patient tissues. HOTAIRM1 silencing showed suppressive effects on the malignant behaviors of glioma cells in vitro and inhibited glioma tumors in vivo.

Insulin-like growth factor binding protein 2 has been revealed to function as an RBP for HOTAIRM1. Previous studies have reported that IGFBP2 facilitates angiogenesis by activating CD144 and MMP2, and its expression is significantly correlated with VM formation in glioma patient samples.[51] Furthermore, *IGFBP2* is an oncogene contributing to glioma progression and is suggested as a potential therapeutic target for gliomas at high grade.[52] In this study, we found that IGFBP2 is significantly upregulated in glioma cells and patient tissues (more significantly upregulated in high grade glioma tissue samples). Insulin-like growth factor binding protein 2 was demonstrated to bind to HOTAIRM1 and was positively regulated by HOTAIRM1. Rescue assays indicated that IGFBP2 overexpression reversed the suppressive effects induced by HOTAIRM1 knockdown on glioma cell malignant behaviors.

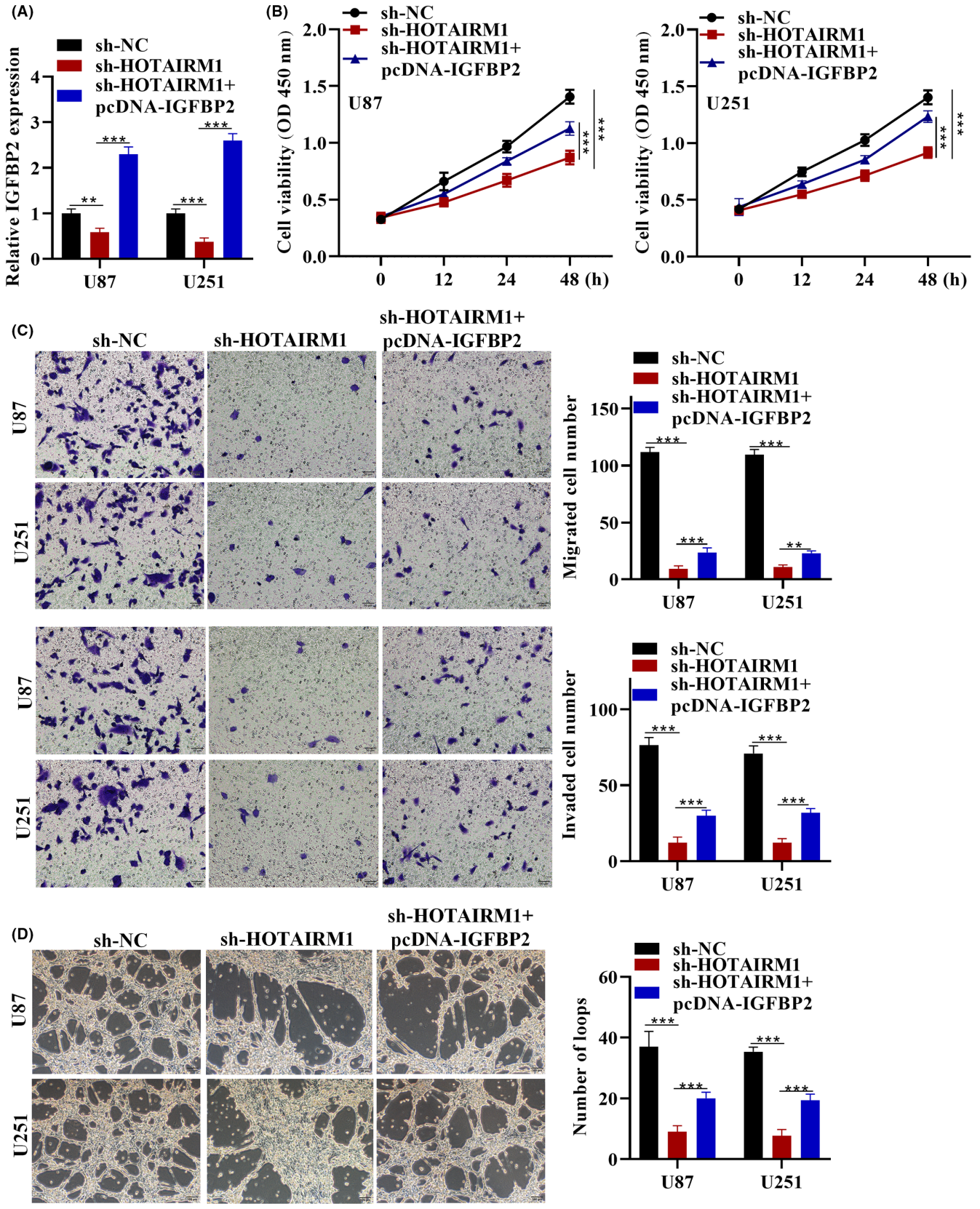

FIGURE 6 Insulin-like growth factor binding protein 2 (IGFBP2) reverses the effects of HOXA transcript antisense RNA myeloid-specific 1 (HOTAIRM1) deficiency on vasculogenic mimicry (VM) in glioma cells. (A) A rescue assay model was successfully established through cell transfection with shRNAs (sh-HOTAIRM1 + pcDNA-IGFBP2) and verified by quantitative RT-PCR. (B) Rescue of HOTAIRM1 deviancy by IGFBP2 complementary expression on glioma cell viability and proliferation by CCK-8 assay. (C) Transwell and tube formation assays after HOTAIRM1 silencing and IGFBP2 rescue. Scale bar, 50 μm. (D) Rescue of HOTAIRM1 deviancy by IGFBP2 complementary expression on VM formation in glioma cells. Scale bar, 100 μm. $^{**}p < 0.01$, $^{***}p < 0.001$. NC, negative control; OD, optical density

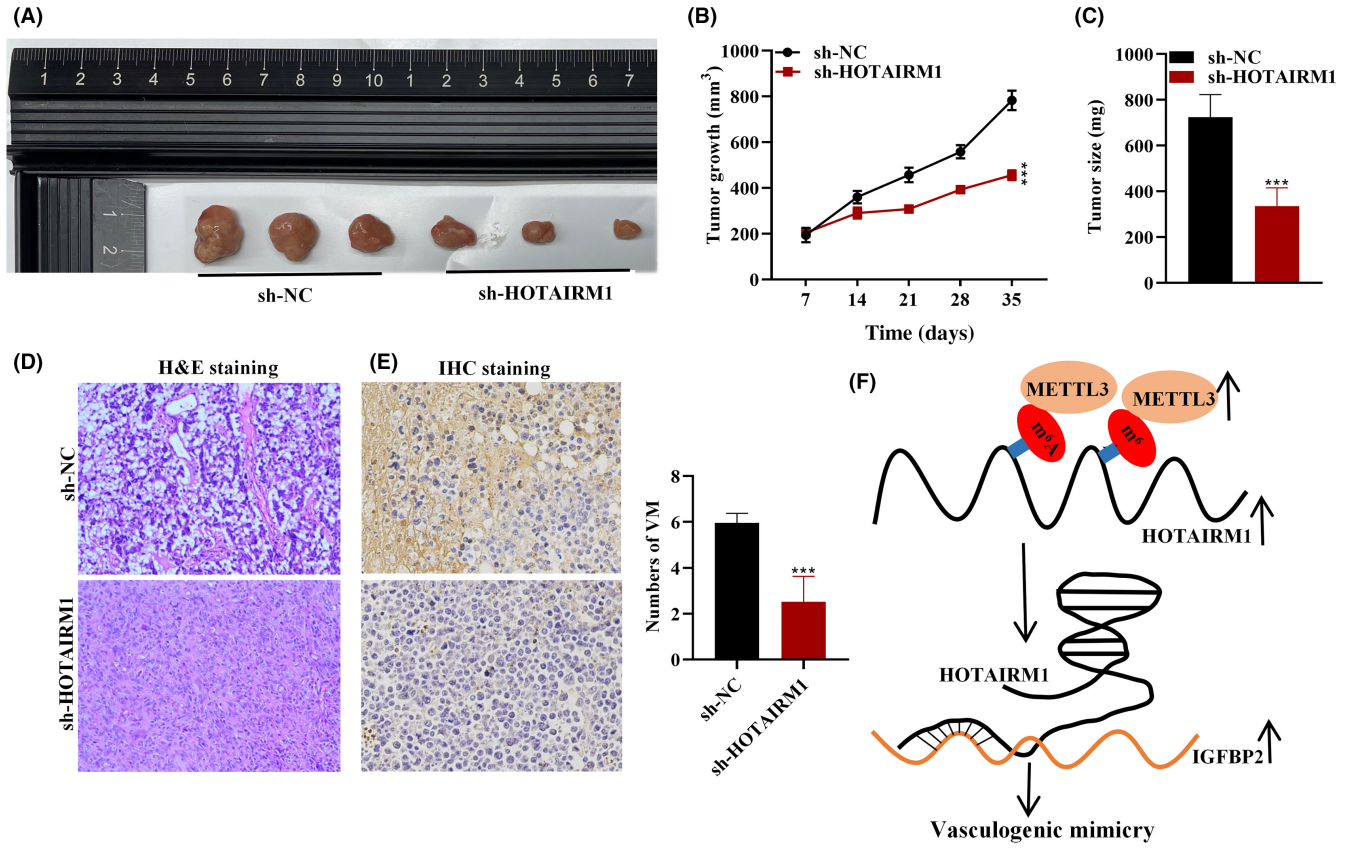

FIGURE 7 HOXA transcript antisense RNA myeloid-specific 1 (HOTAIRM1) deficiency inhibits glioma progression and vasculogenic mimicry (VM) formation in vivo. (A) Images and comparison of glioma xenograft tumors in nude mice between the negative control (sh-NC) and sh-HOTAIRM1 groups. (B, C) Comparison of tumor growth and size in nude mice between the sh-NC and sh-HOTAIRM1 groups. (D) H&E staining for histopathological examination (magnification, 200×). (E) Immunohistochemistry (IHC) assay by the CD31/PAS double staining method for VM detection and scoring (magnification, 200×). (F) Schematic illustration of the potential mechanism by which methyltransferase-like 3 (METTL3)-dependent N6-methyladenosine (m6A)-modified HOTAIRM1 promoted VM by targeting insulin-like growth factor binding protein 2 (IGFBP2) in glioma progression. ***$p < 0.001$

In conclusion, our results revealed that METTL3-dependent m6A-modified HOTAIRM1 promoted cell proliferation, migration, invasion, and VM formation in glioma by upregulating IGFBP2 (Figure 7F). It is critical to understand the m6A-related mechanisms that contribute to VM formation to develop VM-based glioma treatments. The findings of our study could shed new light on targeted therapy for glioma treatment.

AUTHOR CONTRIBUTIONS

ZW and YL were involved in the conception and design of this study. ZW performed the data analysis and interpreted the results. ZW prepared the first draft of the manuscript. YL did a critical revision of the manuscript. YL supervised the study.

ACKNOWLEDGMENT

This work was supported by the Zhejiang Basic Public Welfare Research Program (No. LGF22H160067).

DISCLOSURE

There are no declared conflicts of interest.

DATA AVAILABILITY STATEMENT

The corresponding author can provide the data that support the findings of this study upon request.

ETHICS STATEMENT

Approval of the research protocol by an institutional review board: All experimental procedures were approved by the Ethics Committee of Zhejiang Provincial Tongde Hospital.

Informed consent: Written informed consent was obtained from each participant.

Registry and registration no. of the study/trial: N/A.

Animal studies: The contents of this study are in full compliance with government policy and the Declaration of Helsinki.

ORCID

Yihai Lin https://orcid.org/0000-0003-4790-8318

REFERENCES

1. Wesseling P, Capper D. WHO 2016 Classification of gliomas. *Neuropathol Appl Neurobiol*. 2016;44:139-150.

2. Alifieris C, Trafalis DT. Glioblastoma multiforme: Pathogenesis and treatment. *Pharmacol Ther*. 2015;152:63-82.
3. Kirkpatrick JP, Sampson JH. Recurrent malignant gliomas. *Semin Radiat Oncol*. 2014;24:289-298.
4. de Groot JF, Mandel JJ. Update on anti-angiogenic treatment for malignant gliomas. *Curr Oncol Rep*. 2014;16:380.
5. Weller M, Wick W, Aldape K, et al. Glioma. *Nat Rev Dis Primers*. 2015;1:15017.
6. Chen R, Smith-Cohn M, Cohen AL, Colman H. Glioma Subclassifications and Their Clinical Significance. *Neurotherapeutics*. 2017;14:284-297.
7. Plate KH, Risau W. Angiogenesis in malignant gliomas. *Glia*. 1995;15:339-347.
8. Maniotis AJ, Folberg R, Hess A, et al. Vascular channel formation by human melanoma cells in vivo and in vitro: vasculogenic mimicry. *Am J Pathol*. 1999;155:739-752.
9. Folberg R, Hendrix MJ, Maniotis AJ. Vasculogenic mimicry and tumor angiogenesis. *Am J Pathol*. 2000;156:361-381.
10. Folberg R, Maniotis AJ. Vasculogenic mimicry. *APMIS*. 2004;112:508-525.
11. Morales-Guadarrama G, Garcia-Becerra R, Mendez-Perez EA, Garcia-Quiroz J, Avila E, Diaz L. Vasculogenic mimicry in breast cancer: clinical relevance and drivers. *Cell*. 2021;10:1758.
12. Ayala-Dominguez L, Olmedo-Nieva L, Munoz-Bello JO, et al. Mechanisms of vasculogenic mimicry in ovarian cancer. *Front Oncol*. 2019;9:998.
13. Lizarraga-Verdugo E, Avendano-Felix M, Bermudez M, Ramos-Payan R, Perez-Plasencia C, Aguilar-Medina M. Cancer Stem Cells and Its Role in Angiogenesis and Vasculogenic Mimicry in Gastrointestinal Cancers. *Front Oncol*. 2020;10:413.
14. Cao Z, Bao M, Miele L, Sarkar FH, Wang Z, Zhou Q. Tumour vasculogenic mimicry is associated with poor prognosis of human cancer patients: a systemic review and meta-analysis. *Eur J Cancer*. 2013;49:3914-3923.
15. Zheng N, Zhang S, Wu W, Zhang N, Wang J. Regulatory mechanisms and therapeutic targeting of vasculogenic mimicry in hepatocellular carcinoma. *Pharmacol Res*. 2021;166:105507.
16. Cai H, Liu W, Liu X, et al. Advances and prospects of vasculogenic mimicry in glioma: a potential new therapeutic target? *Onco Targets Ther*. 2020;13:4473-4483.
17. Zhang N, Zuo Y, Peng Y, Zuo L. Function of N6-Methyladenosine Modification in Tumors. *J Oncol*. 2021;2021:6461552.
18. Zheng F, Du F, Zhao J, et al. The emerging role of RNA N6-methyladenosine methylation in breast cancer. *Biomark Res*. 2021;9:39.
19. Lobo J, Barros-Silva D, Henrique R, Jeronimo C. The emerging role of epitranscriptomics in cancer: focus on urological tumors. *Genes (Basel)*. 2018;9:552.
20. Wu W, Zhang F, Zhao J, He P, Li Y. The N6-methyladenosine:mechanisms, diagnostic value, immunotherapy prospec-ts and challenges in gastric cancer. *Exp Cell Res*. 2022;415:113115.
21. Yankova E, Aspris D, Tzelepis K. The N6-methyladenosine RNA modification in acute myeloid leukemia. *Curr Opin Hematol*. 2021;28:80-85.
22. Huang H, Weng H, Chen J. m(6)A Modification in Coding and Non-coding RNAs: Roles and Therapeutic Implications in Cancer. *Cancer Cell*. 2020;37:270-288.
23. Li J, Wang F, Liu Y, Wang H, Ni B. N(6)-methyladenosine (m(6)A) in pancreatic cancer: Regulatory mechanisms and future direction. *Int J Biol Sci*. 2021;17:2323-2335.
24. Chen Y, Miao L, Lin H, Zhuo Z, He J. The role of m6A modification in pediatric cancer. *Biochim Biophys Acta Rev Cancer*. 2022;1877:188691.
25. Qiao K, Liu Y, Xu Z, et al. RNA m6A methylation promotes the formation of vasculogenic mimicry in hepatocellular carcinoma via Hippo pathway. *Angiogenesis*. 2021;24:83-96.
26. Liu X, He H, Zhang F, et al. m6A methylated EphA2 and VEGFA through IGF2BP2/3 regulation promotes vasculogenic mimicry in colorectal cancer via PI3K/AKT and ERK1/2 signaling. *Cell Death Dis*. 2022;13:483.
27. Tao M, Li X, He L, et al. Decreased RNA m(6)A methylation enhances the process of the epithelial mesenchymal transition and vasculogenic mimicry in glioblastoma. *Am J Cancer Res*. 2022;12:893-906.
28. Fu Y, Dominissini D, Rechavi G, He C. Gene expression regulation mediated through reversible m^6A RNA methylation. *Nat Rev Genet*. 2014;15:293-306.
29. Dominissini D, Moshitch-Moshkovitz S, Schwartz S, et al. Topology of the human and mouse m6A RNA methylomes revealed by m6A-seq. *Nature*. 2012;485:201-206.
30. Liu J, Yue Y, Han D, et al. A METTL3-METTL14 complex mediates mammalian nuclear RNA N6-adenosine methylation. *Nat Chem Biol*. 2014;10:93-95.
31. Zeng C, Huang W, Li Y, Weng H. Roles of METTL3 in cancer: mechanisms and therapeutic targeting. *J Hematol Oncol*. 2020;13:117.
32. Wang Q, Chen C, Ding Q, et al. METTL3-mediated m(6)A modification of HDGF mRNA promotes gastric cancer progression and has prognostic significance. *Gut*. 2020;69:1193-1205.
33. Li T, Hu PS, Zuo Z, et al. METTL3 facilitates tumor progression via an m(6)A-IGF2BP2-dependent mechanism in colorectal carcinoma. *Mol Cancer*. 2019;18:112.
34. Chang YZ, Chai RC, Pang B, et al. METTL3 enhances the stability of MALAT1 with the assistance of HuR via m6A modification and activates NF-κB to promote the malignant progression of IDH-wildtype glioma. *Cancer Lett*. 2021;511:36-46.
35. Li D, Chai L, Yu X, et al. The HOTAIRM1/miR-107/TDG axis regulates papillary thyroid cancer cell proliferation and invasion. *Cell Death Dis*. 2020;11:227.
36. Chao H, Zhang M, Hou H, Zhang Z, Li N. HOTAIRM1 suppresses cell proliferation and invasion in ovarian cancer through facilitating ARHGAP24 expression by sponging miR-106a-5p. *Life Sci*. 2020;243:117296.
37. Li Q, Dong C, Cui J, Wang Y, Hong X. Over-expressed lncRNA HOTAIRM1 promotes tumor growth and invasion through up-regulating HOXA1 and sequestering G9a/EZH2/Dnmts away from the HOXA1 gene in glioblastoma multiforme. *J Exp Clin Cancer Res*. 2018;37:265.
38. Chen Y, Lin Y, Shu Y, He J, Gao W. Interaction between N(6)-methyladenosine (m(6)A) modification and noncoding RNAs in cancer. *Mol Cancer*. 2020;19:94.
39. Zhou Y, Zeng P, Li YH, Zhang Z, Cui Q. SRAMP: prediction of mammalian N6-methyladenosine (m6A) sites based on sequence-derived features. *Nucleic Acids Res*. 2016;44:e91.
40. Li JH, Liu S, Zhou H, Qu LH, Yang JH. starBase v2.0: decoding miRNA-ceRNA, miRNA-ncRNA and protein-RNA interaction networks from large-scale CLIP-Seq data. *Nucleic Acids Res*. 2014;42:D92-D97.
41. He L, Li H, Wu A, Peng Y, Shu G, Yin G. Functions of N6-methyladenosine and its role in cancer. *Mol Cancer*. 2019;18:176.
42. Wang T, Kong S, Tao M, Ju S. The potential role of RNA N6-methyladenosine in Cancer progression. *Mol Cancer*. 2020;19:88.
43. Wang S, Chai P, Jia R, Jia R. Novel insights on m(6)A RNA methylation in tumorigenesis: a double-edged sword. *Mol Cancer*. 2018;17:101.
44. Cui Q, Shi H, Ye P, et al. m(6)A RNA Methylation Regulates the Self-Renewal and Tumorigenesis of Glioblastoma Stem Cells. *Cell Rep*. 2017;18:2622-2634.
45. Batista PJ, The RNA. Modification N(6)-methyladenosine and Its Implications in Human Disease. *Genomics Proteomics Bioinformatics*. 2017;15:154-163.
46. Chai RC, Chang YZ, Chang X, et al. YTHDF2 facilitates UBXN1 mRNA decay by recognizing METTL3-mediated m(6)A modification to activate NF-κB and promote the malignant progression of glioma. *J Hematol Oncol*. 2021;14:109.

47. Tassinari V, Cesarini V, Tomaselli S, et al. ADAR1 is a new target of METTL3 and plays a pro-oncogenic role in glioblastoma by an editing-independent mechanism. *Genome Biol*. 2021;22:51.
48. Ahmadov U, Picard D, Bartl J, et al. The long non-coding RNA HOTAIRM1 promotes tumor aggressiveness and radiotherapy resistance in glioblastoma. *Cell Death Dis*. 2021;12:885.
49. Liang Q, Li X, Guan G, et al. Long non-coding RNA, HOTAIRM1, promotes glioma malignancy by forming a ceRNA network. *Aging*. 2019;11:6805-6838.
50. Lin YH, Guo L, Yan F, Dou ZQ, Yu Q, Chen G. Long non-coding RNA HOTAIRM1 promotes proliferation and inhibits apoptosis of glioma cells by regulating the miR-873-5p/ZEB2 axis. *Chin Med J*. 2020;133:174-182.
51. Liu Y, Li F, Yang YT, et al. IGFBP2 promotes vasculogenic mimicry formation via regulating CD144 and MMP2 expression in glioma. *Oncogene*. 2019;38:1815-1831.
52. Moore LM, Holmes KM, Smith SM, et al. IGFBP2 is a candidate biomarker for Ink4a-Arf status and a therapeutic target for high-grade gliomas. *Proc Natl Acad Sci U S A*. 2009;106:16675-16679.

SUPPORTING INFORMATION

Additional supporting information can be found online in the Supporting Information section at the end of this article.

How to cite this article: Wu Z, Lin Y, Wei N. N6-methyladenosine-modified HOTAIRM1 promotes vasculogenic mimicry formation in glioma. *Cancer Sci*. 2023;114:129-141. doi: 10.1111/cas.15578